# Low-Loss Design Method for a Planar Dielectric-Waveguide Y Branch: Effect of a Taper of Serpentine Shape

Mikio Tsuji, *Member, IEEE*, Osamu Tanaka, and Hiroshi Shigesawa, *Senior Member, IEEE*

*Abstract*—**A new design method is proposed for a planar dielectric waveguide Y branch with low loss caused by radiation. In contrast to the usual design methods, in which the generation of the radiation wave is kept as small as possible, the present method positively uses, for the first time, the behavior of such a radiation wave. We intentionally generate the radiation wave at any local position along a taper section of the Y branch, and its power conversion and reconversion with the surface-wave mode are controlled to reduce the insertion loss for the surface-wave mode.**

**A design example shows that the low-loss Y branch should have a serpentine taper, which is an unexpected shape from the usual design point of view. The effectiveness of our design method presented here is confirmed by comparing the numerical results with those of the usual types of Y branches and with measurements.**

## I. Introduction

PLANAR circuits based on open dielectric waveguides have become increasingly important in the past few years in connection with integrated circuits ranging from millimeter-wave to optical frequencies. Of these circuits, the Y branch is one of the basic but most important devices. It is used not only as a power divider and combiner, but also in the active devices for light-intensity modulation and switching. However, the guided wave on a Y branch always loses energy by radiation because of the discontinuous feature of branch structures. Such radiation causes serious problems in circuit performance because of, for example, the undesired power coupling, or crosstalk, with neighboring circuits. Such an effect becomes significant in the millimeter-wave region, because branch circuits must be designed to be as compact as possible to the wavelength even if the junction angle becomes large and the dielectric constant ratio between the core and the surroundings increases.

Many approximate approaches have appeared so far. Sasaki *et al.* [1] estimated radiation loss by neglecting the strong coupling between the branching waveguides in the vicinity of the junction. Burns *et al.* [2] and Yajima [3] calculated mode conversion between the guided modes by the approximate step theory of Marcuse [4], which assumed an approximate orthogonality of modes on one side of an infinitesimal step to the modes on the other side. The volume current method [5] is also an approximate method for calculating the radiation loss. Furthermore, numerical solutions by the beam-propagation method were considered in [6]. Also, certain techniques have been discussed for reducing the insertion loss of curved waveguides [7] and Y branches [8]. None of these studies, however, discussed the design problems of Y branches from the point of view of the accurate behavior of both the surface-wave mode and the radiation wave. They understood that, once the radiation wave is generated, it is scattered to the surroundings and cannot be used in devising low-loss Y branches. According to this view, a low-loss Y branch may be obtained only when the taper shape changes smoothly so that the input surface-wave mode can couple to the radiation wave as little as possible. This idea usually requires a large dimension to the wavelength for the nonuniform taper section, and such a Y branch will not be practical in the millimeter-wave region.

This paper develops, for the first time, a design method of Y branches with amazingly reduced loss from radiation. In a new type of Y branch, the radiation wave is intentionally generated along the taper and is controlled so that it can play an important role in reducing radiation loss (theoretically realizing zero loss).

## II. Theoretical Approach

### A. Physical Consideration

Fig. 1 illustrates the Y branch considered in the analysis. For simplicity, the structure is assumed to be uniform in the $x$ direction, and the fundamental $TE_0$ slab surface-wave mode is incident from left-hand side of the waveguide, as shown. Also, the separation of the output guides II and $\overline{\text{II}}$ is assumed to be sufficiently wide so that their effect on each other can be neglected. We assume further that each guide can support only the fundamental surface-wave mode.

In general, the electromagnetic field in a uniform dielectric waveguide of the open type can be expressed completely by the constituent fields of both the surface-wave modes and the radiation wave (a continuum of modes with the continuous spectrum) [9]. The constituent fields do not couple with each other as long as a waveguide is uniform along the propagation direction. However, if a waveguide becomes nonuniform and/or has discontinuities, power coupling oc-

Manuscript received February 26, 1990; revised July 27, 1990. This work was supported in part by the Ministry of Education, Science and Culture of Japan under a Grant-in-Aid for General Scientific Research (63550261).

M. Tsuji and H. Shigesawa are with the Department of Electronics, Doshisha University, Karasuma-Imadegawa, Kamikyo-ku, Kyoto, 602 Japan.

O. Tanaka was with the Department of Electronics, Doshisha University, Kyoto, 602 Japan. He is now with Hitachi Ltd., Tokyo, Japan.

IEEE Log Number 9040558.

0018-9480/91/0100-0006$01.00 ©1991 IEEE

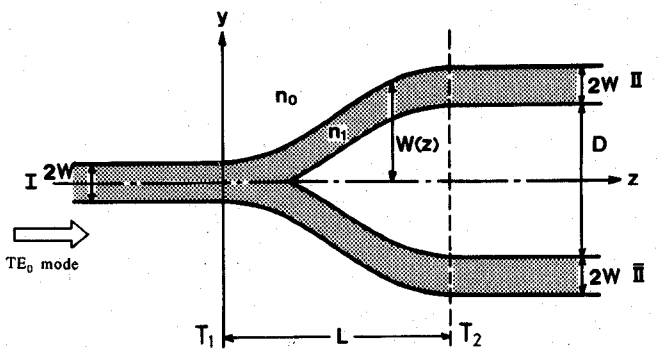


Fig. 1. General configuration of dielectric waveguide Y branch. The structure is uniform in the $x$ direction. The nonuniform structure lies between the terminal planes $T_1$ and $T_2$, which are connected to the input waveguide I and to the output waveguides II, $\overline{\text{II}}$, respectively.

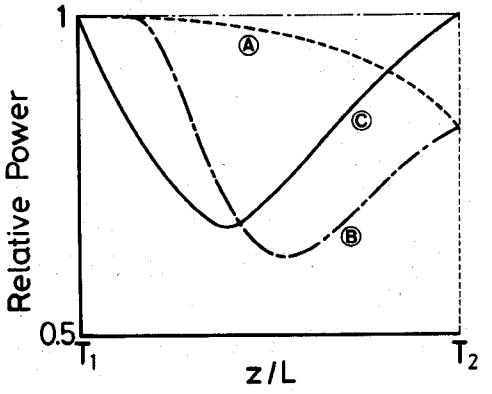


Fig. 2. Conceptual variation of the transmitting power of the surface-wave mode across a plane perpendicular to the $z$ axis.

curs between surface-wave and radiation modes. Papers previously published have considered that a low-loss Y branch is obtained only when the transmitting power of the surface-wave mode is lost gradually along the taper axis and drops monotonically to a certain amount at the output end, marked $T_2$ as shown conceptually by the dashed curve Ⓐ in Fig. 2. This understanding is not correct, as explained below, when a Y branch in the millimeter-wave region is concerned.

It is obvious that the surface-wave mode on a practical Y branch propagates toward the output end, successively repeating, to a greater or lesser degree, the necessary power conversion and reconversion with the radiation modes as well as with the surface-wave mode. Then, it is expected that the power of the surface-wave mode will no longer not change monotonically but rather in a more complex manner. Certainly, a numerical example for the practical linear-taper Y branch discussed in Section III exhibits such a power change, not like curve Ⓐ but like curve Ⓑ in Fig. 2.

Curve Ⓑ in Fig. 2 shows a sudden power conversion into the radiation modes near the input end, and then the power of the radiation modes is again reconverted gradually into the surface-wave mode as they propagate. But, the power drop of the surface-wave mode at the output end $T_2$ is inevitable because a taper shape is decided *a priori*. Therefore, such a Y branch is always accompanied by a loss due to

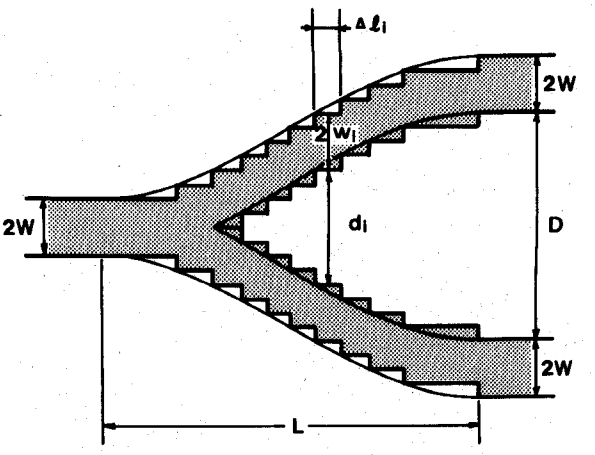


Fig. 3. Step approximation for dielectric waveguide Y branch. Its original shape is indicated by the smooth curve. (The sketch is exaggerated.)

radiation. However, we can obtain a Y branch with theoretically no loss from radiation when the taper shape is designed so as to control *intentionally* the intensive power conversion and reconversion. This will transform part of the input surface-wave mode into the radiation modes with complete control, and we can finally obtain only the desired surface-wave mode in the output waveguide, while the undesired reflection is suppressed at the input end. In such an ideal case, we may expect conceptually the power change shown by the solid curve Ⓒ in Fig. 2.

### *B. Full-Wave Theoretical Approach*

To control intentionally the power conversion and reconversion, it is necessary to solve the wave behavior on a Y branch from the viewpoint of a precise boundary-value problem. This is usually quite difficult for structures of the open type. However, the method we have developed for the analysis of discontinuity problems on open dielectric waveguides is capable of solving this problem. The general approach is presented in [10], but a brief summary with some necessary modifications is in order.

The basis of our approach is to describe the wave behavior of the Y branch with a taper of arbitrary shape by a generalized *equivalent network* which is amenable to the ordinary microwave-network method. For this purpose, we approximate a Y branch by a number of infinitesimal step discontinuities connected in tandem through a uniform dielectric waveguide with a segment length $\Delta l_i$ as shown in Fig. 3. Such an approximated structure is then typically divided into four building blocks as shown in Fig. 4. The first (Fig. 4(a)) is the single homogeneous waveguide with guide width $w_i$, the second (Fig. 4(b)) is the step discontinuity on it, the third (Fig. 4(c)) is the parallel homogeneous waveguide with guide width $w_i$ and separation $d_i$, and the last (Fig. 4(d)) is the step discontinuity.

Let us first consider homogeneous dielectric waveguides. The mathematical development described hereafter is valid for both part (a) and part (c) of Fig. 4 except for the functional form of modal functions. Then in this subsection we assume a general case that $M$ surface-wave modes and the radiation modes polarized in the $x$ direction are travel-

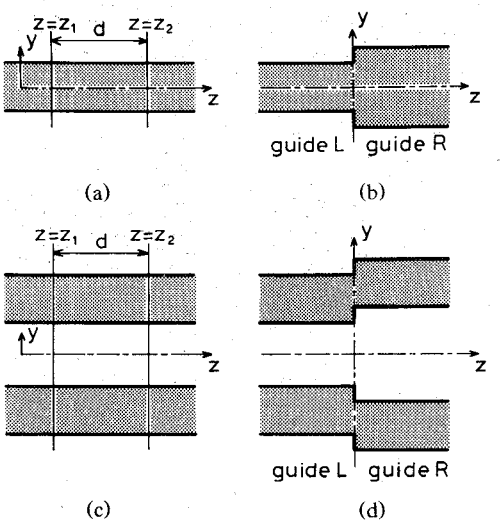


Fig. 4. Four typical types of building blocks for the approximated structure of Fig. 3: (a) the single homogeneous dielectric slab; (b) the step discontinuity on the waveguide shown in (a); (c) the parallel homogeneous dielectric slab; and (d) the step discontinuity on the waveguide shown in (c).

ing to the positive $z$ direction. Then the total electric field $E_x(y,z)$ in the $xy$ plane at an arbitrary $z$ position is completely expressed[1] by the following equation [10]:

$$E_x(y,z) = \sum_{m=0}^{M-1} A_m(z) e_{xm}(y) + \int_0^{n_0k_0} f(\rho,z) e_x(y,\rho)\, d\rho + \int_{n_0k_0}^{\alpha n_0k_0} g(\rho,z) e_x(y,\rho)\, d\rho, \quad (1)$$

where $e_{xm}(y)$ and $e_x(y,\rho)$ are the orthonormal modal functions of the $m$th surface-wave mode and the radiation mode with the transverse wavenumber $\rho$ in the $y$ direction outside the dielectric, respectively. The functional forms of these modal functions do not change as they propagate along a homogeneous waveguide, but their complex root-power amplitude $A_m(z)$ and the continuous spectral amplitudes $f(\rho,z)$ for propagating radiation modes $(0<\rho<n_0k_0)$ and $g(\rho,z)$ for nonpropagating radiation modes $(n_0k_0<\rho<\alpha n_0k_0)$ do change. The change in each complex amplitude of surface-wave modes is easily pictured by the simple network model consisting of an uncoupled transmission line, even for a dielectric waveguide of the open type. Such a network model is not valid for radiation modes at all, because each radiation mode is not an eigenmode and its power intensity is indefinite.

Nevertheless, we intend to initiate a network model effective for radiation modes consistent with the network model for surface-wave modes mentioned above. To this end, let us expand the spectral functions $f(\rho,z)$ and $g(\rho,z)$ into (practically truncated) series of the orthonormal functions $\phi_n(\rho)$ and $\psi_n(\rho)$ defined in their own $\rho$ regions with the unknown coefficients $A_{M+n}(z)$ and $A_{M+N+n}(z)$, $(n=1,2,\cdots,N)$, respectively, as seen in [10]. Then we can recompose the radiation modes to have a discrete set of an infinite number of *spectral composite modes*, defined by

$$\tilde{e}_{xn}(y) = \int_0^{n_0k_0} \phi_n(\rho) e_x(y,\rho)\, d\rho$$

$$\hat{e}_{xn}(y) = \int_{n_0k_0}^{\alpha n_0k_0} \psi_n(\rho) e_x(y,\rho)\, d\rho. \quad (2)$$

We can rewrite the total electric fields $E_x(y,z_i)$ of (1) on the planes at $z=z_i$ $(i=1,2)$, and they are completely expressed by the following equations:

$$E_x(y,z_1) = \sum_{m=0}^{M-1} A_m(z_1) e_{xm}(y) + \sum_{n=0}^{N-1} \left[ A_{M+n}(z_1)\tilde{e}_{xn}(y) + A_{M+N+n}(z_1)\hat{e}_{xn}(y) \right] \quad (3)$$

$$E_x(y,z_2) = \sum_{m=0}^{M-1} B_m(z_2) e_{xm}(y) + \sum_{n=0}^{N-1} \left[ B_{M+n}(z_2)\tilde{e}_{xn}(y) + B_{M+N+n}(z_2)\hat{e}_{xn}(y) \right]. \quad (4)$$

As is well known, the amplitude $B_m(z_2)$ is related to $A_m(z_1)$ by $B_m(z_2)=A_m(z_1)\exp(-j\beta_m d)$, where $\beta_m$ is the phase constant of the $m$th surface-wave mode, and $d=z_2-z_1$. In contrast to this, the complex amplitude, for example, $A_{M+n}(z_1)$ of the $n$th spectral composite mode, changes as it propagates and there is no longer a one-to-one correspondence between $A_{M+n}$ and $B_{M+n}$ or $A_{M+N+n}$ and $B_{M+N+n}$. Instead, one of the input spectral composite mode on a local plane at $z=z_1$ necessarily couples with all of the propagating or nonpropagating output spectral composite modes on a different local plane at $z=z_2$. As a result, with have the following relations:

$$B_{M+n}(z_2) = \sum_{p=0}^{N-1} \tilde{S}_{np}(d)\, A_{M+p}(z_1) \quad (5)$$

$$B_{M+N+n}(z_2) = \sum_{p=0}^{N-1} \hat{S}_{np}(d)\, A_{M+N+p}(z_1) \quad (6)$$

where

$$\tilde{S}_{np}(d) = \int_0^{n_0k_0} \phi_n(\rho)\phi_p(\rho) \exp(-j\beta(\rho)d)\, d\rho \quad (7)$$

$$\hat{S}_{np}(d) = \int_{n_0k_0}^{\alpha n_0k_0} \psi_n(\rho)\psi_p(\rho) \exp(-\gamma(\rho)d)\, d\rho. \quad (8)$$

The quantities $\beta(\rho)=\sqrt{(n_0k_0)^2-\rho^2}$ and $\gamma(\rho)=j\beta(\rho)$ are the phase constants of the propagating and nonpropagating radiation modes, respectively.

If any field distribution given at $z=z_2$ propagates in the negative $z$ direction, the resultant field at $z=z_1$ can be expressed by relations (5) and (6). The equivalent network for a homogeneous dielectric waveguide of length $d$ can be represented by Fig. 5, of which terminal amplitudes are governed by the $S$ matrix $[S_{\mathrm{LINE}}]$ (see [10, appendix II]).

Next, let us derive the $S$ matrix for the equivalent network of a step discontinuity between the two semi-infinite homogeneous waveguides shown in parts (b) and (d) of Fig. 4 on the basis of the spectral composite modes in conjunction with surface-wave modes. We consider that one of these modes is incident from the left-hand side (guide L) or the right-hand side (guide R). An example of such excitation is

[1]Here $\alpha$ is an optimally chosen parameter to limit the branch-cut integral in practical cases (see [11] for details).

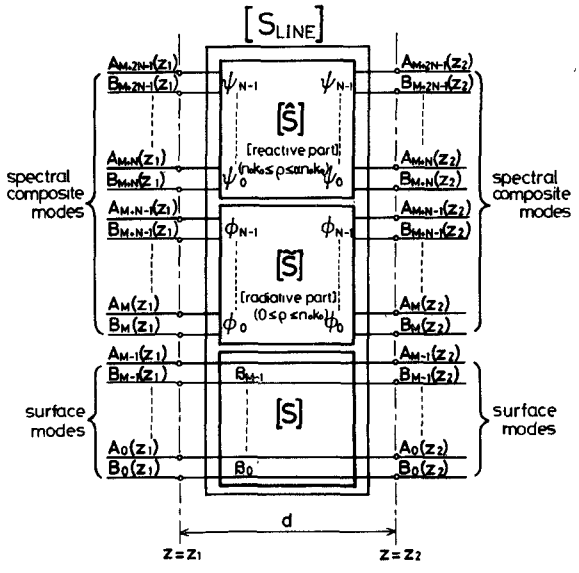


Fig. 5. Equivalent network representation for the homogeneous slab waveguide, where the scattering matrix $[S_{\mathrm{LINE}}]$ consists of the three elementary matrices $[S]$, $[\tilde{S}]$, and $[\hat{S}]$, corresponding, respectively, to the surface-wave modes, the propagating spectral composite modes, and the nonpropagating spectral composite modes.

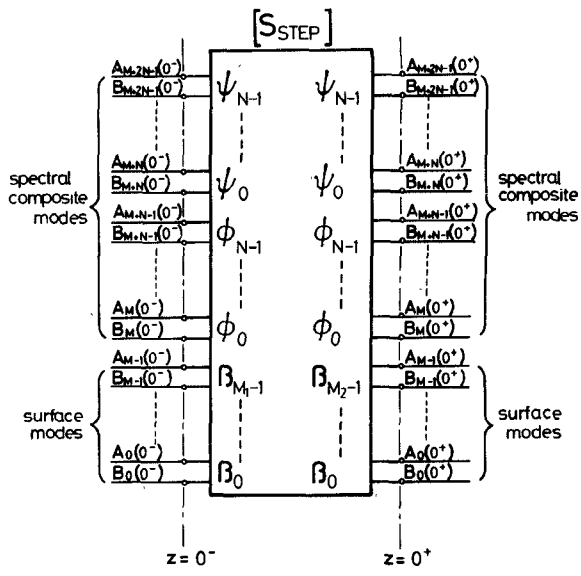


Fig. 6. Equivalent network representation for the step discontinuity shown in Fig. 4(b) or (d).

the incidence of the $q$th surface-wave mode from the left-hand side. Then, the electric fields tangential to the discontinuity plane can be expressed as follows:

$$E_x^{\mathrm{L}}(y,0_-) = \sum_{p=0}^{M+2N-1} (\delta_{pq} + R_{pq}) e_{xp}^{\mathrm{L}}(y) \qquad (9)$$

$$E_x^{\mathrm{R}}(y,0_+) = \sum_{p=0}^{M+2N-1} T_{pq} e_{xp}^{\mathrm{R}}(y) \qquad (10)$$

where the function $e_{xp}^{i}(y)$ ($i = \mathrm{L}$ or R) denotes the modal functions for the surface-wave modes, and the propagating and nonpropagating spectral composite modes on the guide L or R, corresponding to the particular range of the subscript number $p$. The unknown coefficients $R_{pq}$ and $T_{pq}$ in (9) and (10) are then solved by the mode-matching method to fulfill the boundary condition on the junction plane in the sense of least mean squares [10]–[12]. Applying the same procedure to all of the other excitation cases, one can obtain all of the unknown coefficients $R_{pq}$ and $T_{pq}$ which are linked with the elements of the step-discontinuity matrix $[S_{\mathrm{STEP}}]$ (see [10, appendix III]). As a result, a step discontinuity can be expressed by the equivalent network of Fig. 6, which again has the terminal ports corresponding to each of the surface-wave and spectral composite modes.

Let us go back to the problem of Fig. 3. This approximated structure for Fig. 1 is understood as the cascade connection of all of the building blocks shown in Fig. 4, and the complete equivalent network can be expressed as shown in Fig. 7. When the $\mathrm{TE}_0$ fundamental surface-wave mode is the only mode incident from the left-hand side of the structure (as shown), all of the terminal ports, except for the input port of the incident surface-wave mode, should be terminated properly by the corresponding characteristic impedance of each surface-wave mode or each spectral composite mode (see [10, appendix IV]).

The network parameters expressing completely each of the elementary networks can be controlled by varying each of the guide widths $w_i$, the separation widths of parallel waveguides $d_i$, and the segment lengths $\Delta l_i$ ($i = 1,2,\cdots,K$). As was assumed at the beginning of this paper, the only surface-wave mode on each output waveguide II or $\overline{\mathrm{II}}$ is approximately the $\mathrm{TE}_0$ mode, so that the surface-wave field on the branched output waveguide is mathematically expressed by the fundamental even TE-surface-wave mode on a parallel dielectric slab. The insertion loss between input and output surface-wave modes is then expressed as a function of the variables $\{w_i, d_i, \Delta l_i\}$ ($i = 1,2,\cdots,K$), and they are solved by minimizing (ideally by making zero) the insertion loss at a given frequency by using a nonlinear optimization procedure. In this calculation, we set the constraint conditions that the resultant field transforms only into the desired surface-wave mode on the output waveguide with zero insertion loss, while keeping the total length $L$ of the Y branch and the separation width $D$ of two waveguides at the output end constant.

## III. Numerical Results and Experiments

In this section, we design a low-loss Y branch and compare the numerical results first with those of usual types of Y branches, and then with some measurements that we took. In a practical design, we fix all of the guide widths $w_i$ to $W$ and the separation width $D$ at the output end to $10W$. For the sake of experimental convenience, a design is tried at the X band, by using polyethylene ($\epsilon_r = 2.25$) as a dielectric material.

First, to check the validity of a step approximation for a Y branch, the number of steps $K$ is varied in the calculations of the reflection power, the branching transmission power of the surface-wave mode, and the forward and backward radiation powers. Parts (a) and (b) of Fig. 8 show the results for the linear-taper Y branch given by $L = 15W$ and $k_0 W = 1$, where $k_0 = 2\pi/\lambda_0$. It is obvious from this example that the calculated results almost converge when $K > 48$. Therefore, the calculations below are performed with $K = 48$. A total

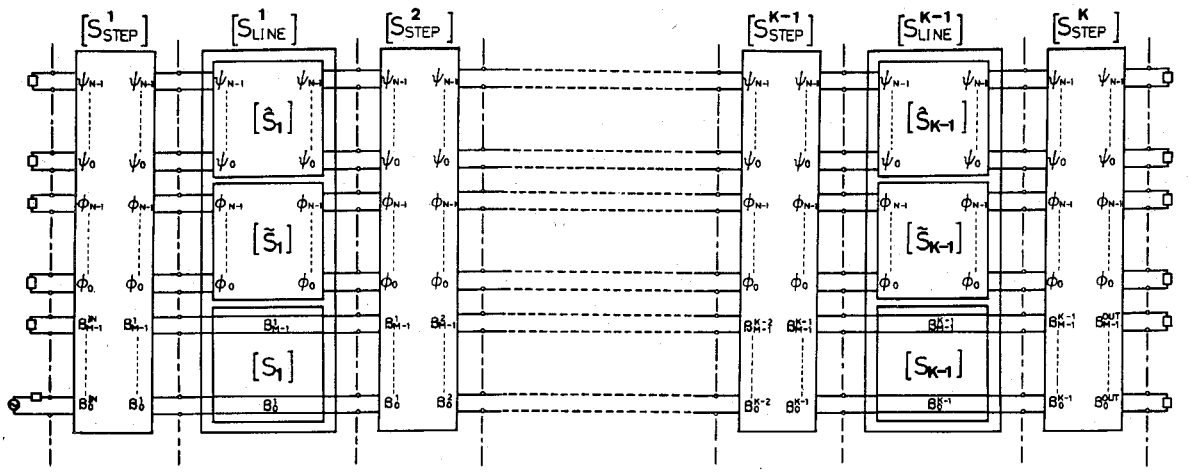


Fig. 7. Equivalent network representation for dielectric waveguide Y branch with an arbitrarily shaped taper. The network parameters are controlled by varying each guide width $w_i$, the separation width of parallel waveguides $d_i$, and segment lengths $\Delta l_i$.

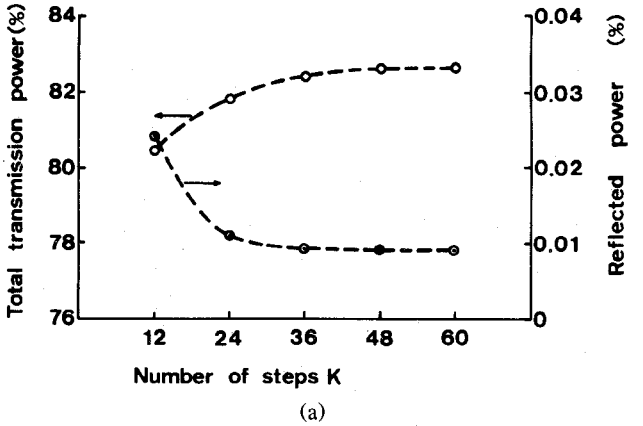


(a)

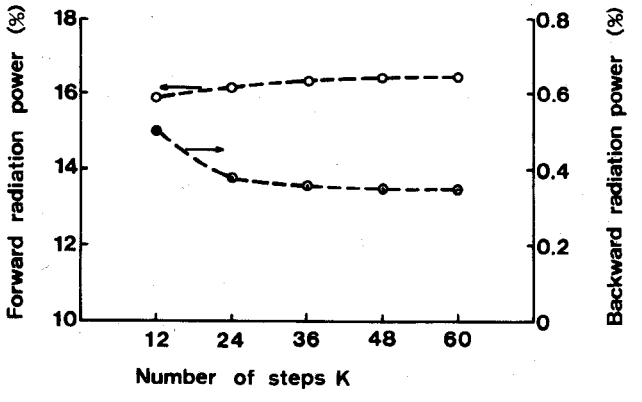


(b)

Fig. 8. Convergence check of the calculated powers as a function of the number of steps $K$ for the linear-taper Y branch with the dimension of $L/W = 15$ and $k_0W = 1$. (a) The powers of the surface-wave mode. (b) The powers of the radiation wave.

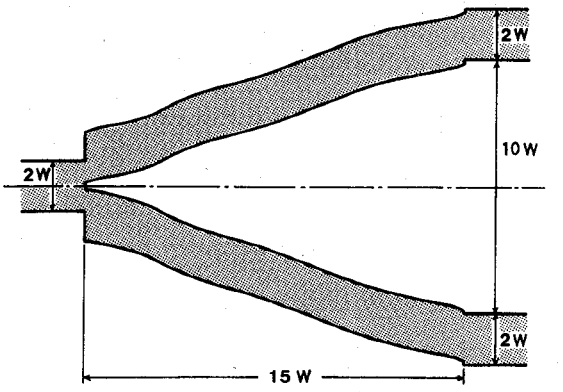


(a)

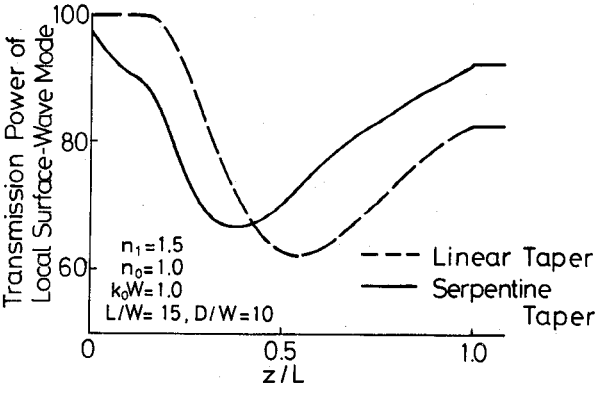


(b)

Fig. 9. Characteristic features of the low-loss Y branch synthesized at $k_0W = 1$. (a) Configuration of the low-loss Y branch (not exaggerated, but enlarged in its scale). (b) Curve of the calculated power change of the surface-wave mode with the comparative one for the linear-taper Y branch.

power conservation of greater than 99.5% is then obtained in the calculations.

Next, we synthesize a low-loss Y branch at $k_0W = 1$ by varying each of the segment lengths $\Delta l_i$ while keeping $L = 15W$. The lengths $\Delta l_i$ are then solved by the modified Newton iteration method. Fig. 9(a) shows the Y branch synthesized at 9.55 GHz (which corresponds to $k_0W = 1$ when $W = 5$ mm). This configuration consists of the serpentine taper and the abrupt step at both input and output ends. This result indeed seems to be an unexpected one from the usual design point of view, but the prudential physical consideration explains that this result is certainly consistent with

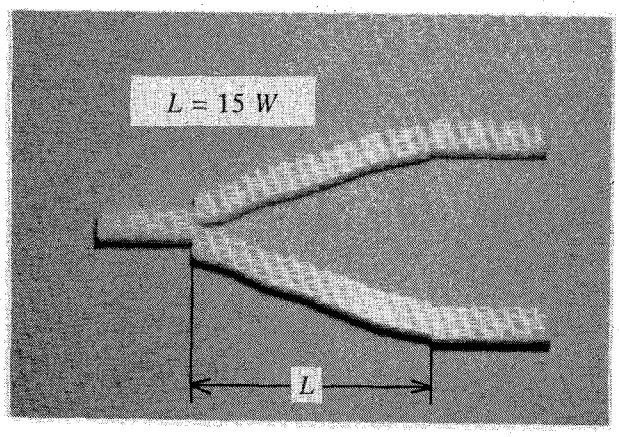


(a)

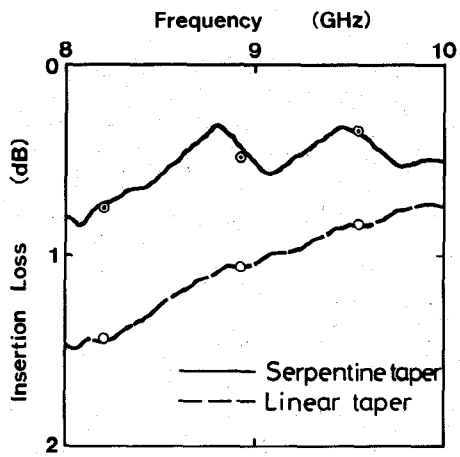


(b)

Fig. 10. (a) External view of a synthesized Y-branch for test and (b) curves of the insertion loss as a function of frequency for the synthesized Y branch and for the linear-taper Y branch. The optimum design is performed at $f = 9.55$ GHz.

our original idea. For example, the solid curve in Fig. 9(b) shows the calculated power change of the local surface-wave mode for the synthesized Y branch, while the dashed curve shows that for the linear-taper Y branch which has the same dimensions as Fig. 9(a) except that the serpentine taper is replaced by a linear taper. As expected, the synthesized Y branch certainly improves the power drop of the surface-wave mode at the output end, and exhibits the low-loss nature. But, the solid curve is somewhat different from that of the ideal case Ⓒ in Fig. 2 and there is a small amount of residual loss. This can be removed when each of the guide widths $w_i$ is also considered as a variable along with $\Delta l_i$ and the taper is approximated by a larger number of segments in the design procedure. However, the computing time increases, and the design cost becomes a bit high.

We performed a set of measurements on a synthesized Y branch at $f = 9.55$ GHz. The dielectric was polyethylene, with $n_1 = 1.5$; the guide width $W$ was 5 mm, the length of the taper section was $L = 15W = 75$ mm, and the branch was made by a numerically controlled machine. This test branch was placed in a parallel-plate waveguide with separation of 8 mm to simulate a two-dimensional structure. An external view of a synthesized Y branch for test is shown in Fig. 10(a). Fig. 10(b) shows the measured insertion loss characteristics

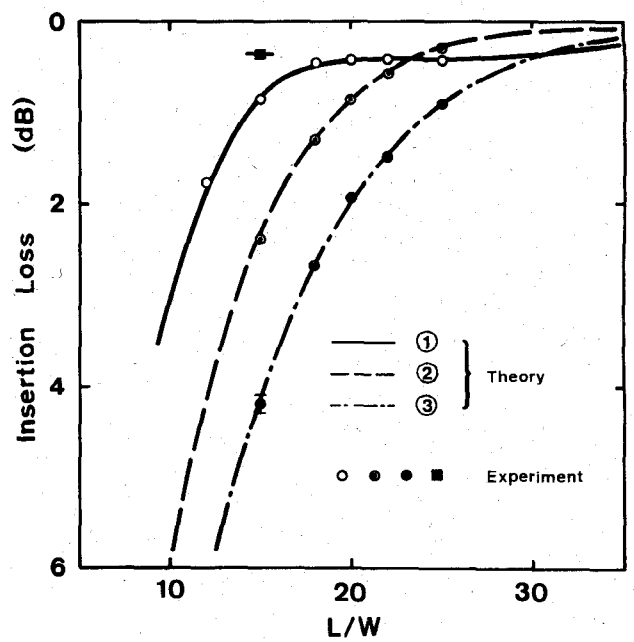


Fig. 11. Calculated and measured insertion loss as a function of the normalized taper length $L/W$ for the Y branches with the linear taper ①, the raised-cosine taper ②, and the integrated raised-cosine taper ③. The square mark on $L/W = 15$ indicates the insertion loss of the synthesized Y branch.

as a function of frequency. The dotted circles indicate the calculations for the Y branch of Fig. 9(a), while the solid curve shows the measured characteristic. It is seen that the agreement is excellent and the fractional power of 93% of the input surface-wave mode is transmitted to the surface-wave mode on the output waveguides. This corresponds to an insertion loss of about 0.32 dB at $f = 9.55$ GHz. Fig. 10(b) also presents another set of calculations and experiment. The single circles indicate the calculation for the linear-taper Y branch which has the same dimension with that of Fig. 9(a). In this case, the insertion loss at $f = 9.55$ GHz is about 0.85 dB, which is 2.7 times worse than the insertion loss of the serpentine taper Y branch. We can also confirm that the serpentine taper Y branch shows low-loss characteristics over a wide frequency range, although the optimization is performed at the frequency $f = 9.55$ GHz.

We have also investigated the Y branches with the raised-cosine and integrated raised-cosine tapers for which the first and the second derivatives are continuous at the junction points, respectively. These are often used in the optical region. Fig. 11 shows the calculated and measured characteristics of the insertion loss as a function of the normalized taper length $L/W$ along with those for the linear-taper Y branch. For comparison, the measured loss of the synthesized low-loss Y branch at $L/W = 15$ is also shown by the square mark. It is seen from these results that the radiation loss of the raised-cosine and integrated raised-cosine taper Y branches is much larger than that of the linear taper when they are designed compactly to the wavelength, for example, in the region of $L/W < 20$. This is understood from the fact that, since the design idea of such Y branches undertakes only a smooth mode conversion between surface-wave modes on the input or the output waveguide and those on the taper section. A larger loss is inevitable when the total length of a

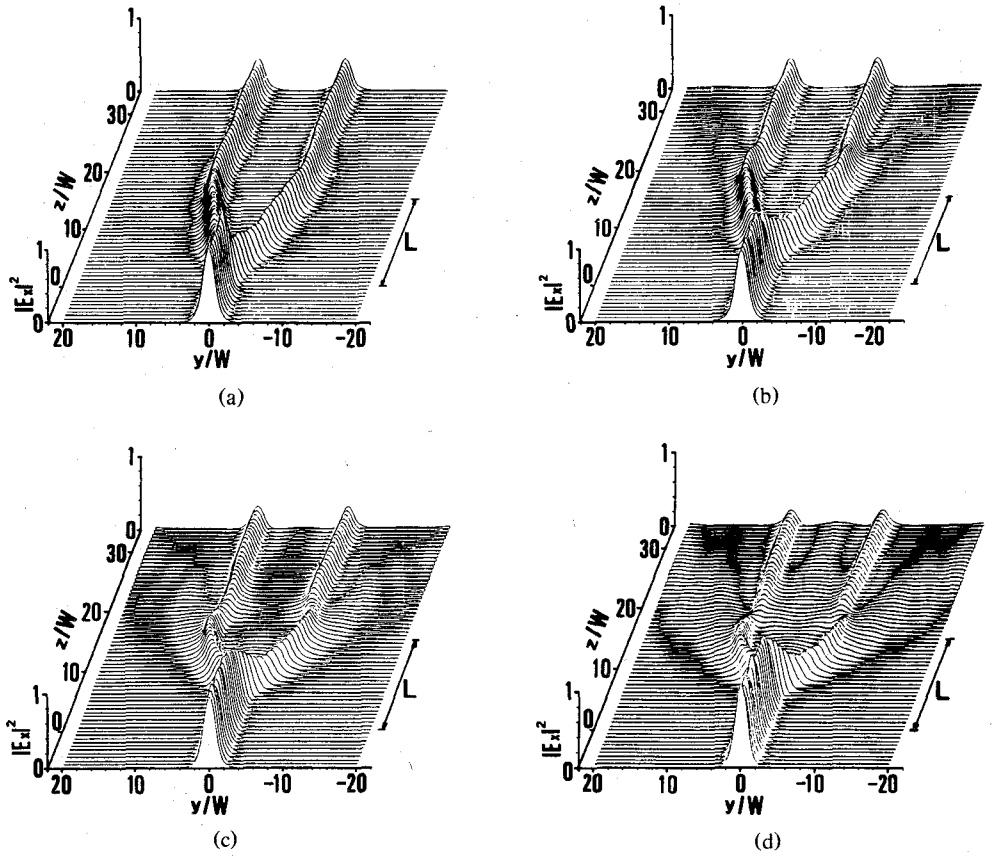


Fig. 12. Field intensity distribution around the taper section when only the surface-wave mode is incident from the $-z$ direction and $L/W = 15$: (a) The synthesized serpentine taper Y branch; (b) the linear-taper Y branch; (c) the raised-cosine taper Y branch; and (d) the integrated raised-cosine taper Y branch.

Y branch is shortened and the bend around the junctions becomes sharp.

The low-loss nature of the serpentine taper Y branch is also confirmed from the wave behavior around the taper section. Fig. 12(a) shows the field intensity distribution for the serpentine taper Y branch with $L/W = 15$, while parts (b), (c), and (d) of Fig. 12 show the distributions for the Y branches with linear taper, raised-cosine taper, and integrated raised-cosine taper of the same $L/W$, respectively. It is clearly seen that the serpentine taper Y branch smoothly transforms the input surface-wave mode into the surface-wave mode on the output waveguide with the help of the local radiation wave, as we expected. In contrast to this, Y branches with conventional tapers scatter the radiation wave away from the Y branch. This tendency is remarkable for the case of tapers with a smooth transition on their configurations, such as the raised-cosine type tapers. Consequently, the method proposed here can evidently be very effective for designing low-loss Y branches in the millimeter-wave region.

## IV. Conclusion

Although two-dimensional structures are discussed here, we have also been successful in applying the design method developed here to practical three-dimensional dielectric-waveguide (e.g., dielectric image-guide) Y branches with the help of an unprecedented method for structural approximation [13]. It is obvious that the idea presented in this paper can also be effective for devising low-loss branch components in planar printed-circuit waveguides, for example, microstrip lines, slotlines, and coplanar waveguides. These results will be presented in a future paper.

## References

[1] H. Sasaki and I. Anderson, "Theoretical and experimental studies on active Y-junctions in optical waveguides," *IEEE J. Quantum Electron.*, vol. QE-14, pp. 883–892, Nov. 1978.

[2] W. K. Burns and A. F. Milton, "Mode conversion in planar-dielectric separating waveguides," *IEEE J. Quantum Electron.*, vol. QE-11, pp. 32–39, Jan. 1975.

[3] H. Yajima, "Coupled mode analysis of dielectric planar branching waveguides," *IEEE J. Quantum Electron.*, vol. QE-14, pp. 749–755, Oct. 1978.

[4] D. Marcuse, "Radiation loss of tapered dielectric slab waveguides," *Bell Syst. Tech. J.*, vol. 49, pp. 273–290, 1970.

[5] M. Kuznetsov and H. A. Haus, "Radiation loss in dielectric waveguide structures by volume current method," *IEEE J. Quantum Electron.*, vol. QE-19, pp. 1505–1514, Oct. 1983.

[6] J. A. Fleck, J. R. Morris and M. D. Feit, "Time-dependence propagation of high energy laser beam through the atmosphere," *Appl. Phys.*, vol. 10, pp. 129–160, June 1976.

[7] L. M. Johnson and D. Yap, "Theoretical analysis of coherently coupled optical waveguide bends," *Appl. Opt.*, vol. 23, pp. 2988–2990, 1984.

[8] O. Hanaizumi, M. Miyagi, M. Minakata, and S. Kawakami, "Antenna coupled Y junction in 3-dimensional dielectric optical waveguides," in *IOOC-ECOC Tech. Dig.*, Oct. 1985, pp. 179–182.

[9] D. Marcuse, *Light Transmission Optics*. New York: Van Nostrand Reinhold, 1972, sec. 8.4.
[10] H. Shigesawa and M. Tsuji, "A new equivalent network method for analyzing discontinuity properties of open dielectric waveguides," *IEEE Trans. Microwave Theory Tech.*, vol. 37, pp. 3–14, Jan. 1989.
[11] H. Shigesawa and M. Tsuji, "Mode propagation through a step discontinuity in dielectric planar waveguide," *IEEE Trans. Microwave Theory Tech.*, vol. MTT-34, pp. 205–212, Feb. 1986.
[12] K. Morishita, S. Inagaki, and N. Kumagai, "Analysis of discontinuities in dielectric waveguides by means of the least squares boundary residual method," *IEEE Trans. Microwave Theory Tech.*, vol. MTT-27, pp. 310–315, Apr. 1979.
[13] M. Tsuji and H. Shigesawa, "Challenge to 3-D discontinuous dielectric waveguide circuit analysis," in *1988 IEEE MTT-S Int. Microwave Symp. Dig.* (New York, NY), May 25–27, 1988, pp. 635–638.

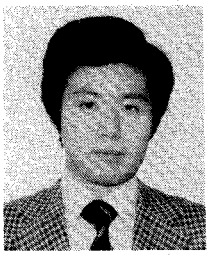

**Mikio Tsuji** (S'78–M'81) was born in Kyoto, Japan, on September 10, 1953. He received the B.E., M.E., and D.E. degrees from Doshisha University, Kyoto, Japan, in 1976, 1978, and 1985, respectively.

Since 1981, he has been with Doshisha University, where he is now an Associate Professor. His present research activities are concerned with millimeter- and submillimeter-wave guiding structures and devices and scattering problems of electromagnetic waves.

Dr. Tsuji is a member of the Institute of Electronics, Information and Communication Engineers of Japan and the Institute of Electrical Engineers of Japan.

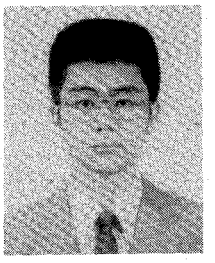

**Osamu Tanaka** was born in Kyoto, Japan, on August 6, 1964. He received B.E. and M.E. degrees from Doshisha University, Kyoto, Japan, in 1987 and 1989, respectively.

He is now with Hitachi Ltd., Tokyo, Japan. Mr. Tanaka is a member of the Institute of Electronics, Information and Communication Engineers of Japan.

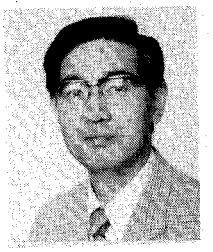

**Hiroshi Shigesawa** (S'62–M'63–SM'85) was born in Hyogo, Japan, on January 5, 1939. He received the B.E., M.E., and D.E. degrees from Doshisha University, Kyoto, Japan, in 1961, 1963, and 1969, respectively.

Since 1963, he has been with Doshisha University. From 1979 to 1980, he was a Visiting Scholar at the Microwave Research Institute, Polytechnic Institute of New York, New York, NY. Currently, he is a Professor in the Faculty of Engineering at Doshisha University. His present research activities involve millimeter- and submillimeter-wave guiding structures and devices and scattering problems of electromagnetic waves.

Dr. Shigesawa is a member of the Institute of Electronics, Information and Communication Engineers of Japan, the Institute of Electrical Engineers of Japan, and the Optical Society of America.